ELSEVIER

European Journal of Pharmaceutics and Biopharmaceutics 50 (2000) 293–300

European Journal of Pharmaceutics and Biopharmaceutics

www.elsevier.com/locate/ejphabio

Research paper

Three-dimensional modeling to determine properties of tableting materials on rotary machines using a rotary tableting machine simulator

Katharina M. Picker*

Martin-Luther-University Halle-Wittenberg, Institute of Pharmaceutical Technology and Biopharmacy, Halle/Saale, Germany

Received 6 January 2000; accepted in revised form 4 May 2000

Abstract

A new three-dimensional modeling technique of tableting data has been used for data measured with a rotary tableting machine simulator. The use of the tableting machine simulator is helpful in this case because a scale up or a change of equipment is easily possible. The model substances used were hydroxypropyl methylcellulose (HPMC 15.000), microcrystalline cellulose (Avicel PH 101), dicalcium phosphate dihydrate (Emcompress) and theophylline monohydrate, four very differently deforming substances. Tablets were produced by simulating a Manesty Betapress with 100 rev./min. The materials were tableted to five graded maximum relative densities ($\rho_{rel,\ max}$) of 0.75, 0.80, 0.85, 0.90 and 0.95. A twisted plane was fitted to the measured data and three parameters: *d*, the time-plasticity: *e*, the pressure plasticity and ω, the elastic decompression, resulted for each material at the given $\rho_{rel,\ max}$ according to the three-dimensional tableting technique. The results show different parameter-plots for the tableting materials, allowing to differentiate between the tableting characteristics of various substances. Three-dimensional modeling of data from rotary machines is shown to be a valuable tool not only for material characterization on eccentric machines but on rotary tableting machines as well.

Keywords: Tablets; Compaction; Data modeling; Curve fitting; Rotary machine

1. Introduction

Mathematical modeling of tableting data has been shown to be a useful method to describe and quantify the deformation and densification properties of materials. During the past, tablet formulations and materials have been usually characterized by different mathematical models using either pressure-displacement [1–6] or pressure–time curves [7–10]. Parameters describing the plasto–elasticity of the substances have been calculated using the change of porosity as a factor of pressure or the ratio of compression to decompression. The last one can be expressed either by the shape of the pressure–time plots or by the ratio of areas under the plots. The areas of force-displacement measurements have been calculated and quantified. Only the viscoelasticity models [11,12] used all three measured variables (time, force and displacement) in the analysis. However, these models resulted in complicated equations with many parameters.

1.1. Theoretical background

1.1.1. Three-dimensional modeling

Another method using all three variables is a new three-dimensional modeling technique [13] by which a twisted plane is fitted to the modified data using normalized time, pressure and porosity according to Heckel, ln $(1/1 - D_{rel})$ (Fig. 1) [1,2]. The equation is like follows

$$y = \ln\left(\frac{1}{1 - D_{rel}}\right) = ((t - t_{max})(d + \omega \cdot p_{max} - p)) + (e \cdot p) + (f + d \cdot t_{max}) - \omega \quad (1)$$

where D_{rel} is relative density, t is time and p is pressure.

$$d = \frac{\partial\left(\ln\left(\frac{1}{1 - D_{rel}}\right)\right)}{\partial t}, \quad e = \frac{\partial\left(\ln\left(\frac{1}{1 - D_{rel}}\right)\right)}{\partial p},$$

$$f = \ln\left(\frac{1}{1 - D_{rel}}\right)$$

$t_{max} =$ time at maximum pressure, $p_{max} =$ the maximum pressure and $\omega =$ the angle of rotation and $D_0 = D_{rel}$ at $t = 0$.

Important parameters have been calculated from this plane: *d*, the slope of porosity over time called 'time plas-

* Martin-Luther-University Halle-Wittenberg, Institute of Pharmaceutical Technology and Biopharmacy, Wolfgang-Langenbeck-Strasse 046120 Halle/Saale, Germany. Tel.: +49-345-552 5138; fax: +49-345-552 7029.

E-mail address: picker@pharmazie.uni-halle.de (K.M. Picker).

0939-6411/00/$ - see front matter
PII: S0939-6411(00)00105-3

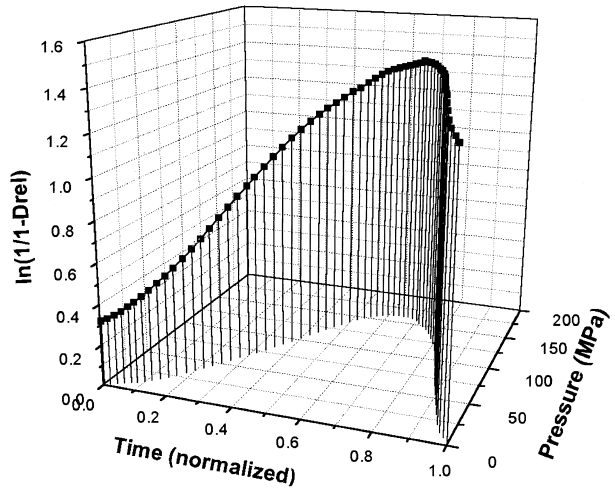

Fig. 1. Three-dimensional data-plot for one compaction cycle of microcrystalline cellulose at $\rho_{rel,\ max}$ of 0.95.

ticity', *e*, the slope of porosity over pressure called 'pressure plasticity' and ω, the angle of rotation at an axis at the time of maximum pressure, called 'fast elastic decompression'. The time plasticity *d* describes the extent of densification over time. A fast deforming material had a high value of *d*, a slow deforming material had a low value of *d*. The value *d* is also reduced when a fast deforming material shows a lot of decompression [13]. This parameter will be different on rotary machines compared with eccentric tableting machines because the time performance is totally different. The parameter *e* gives information on deformation due to pressure. An easily without a lot of pressure deforming material showed a high value of pressure plasticity *e*, a material which needs a lot of pressure showed a low value of *e*. This parameter is similar to the slope of the Heckel function at 'zero pressure' [2]. However, a real direct comparison of *e* and the slope of the Heckel function is not possible because the range of fitting has to be chosen differently in three-dimensional modeling as explained in the experimental section. The parameter *f* is the intersection with the *y*-axis $\ln(1/1 - D_{rel})$. This parameter contains different influences which are in *d* and *e* also, it will be therefore neglected. Finally, the twisting angle ω has to be interpreted. ω describes the angle of rotation at an axis at the time of the maximum pressure. Thus, it describes the twist of compression to decompression phase and thus the extent of decompression. It was called 'fast elastic decompression'. It is the correction of *d* due to pressure. The model is able to differentiate between the influence of pressure and time on the densification process of a material as shown for eccentric tableting machines. The results have been successfully used to characterize the tableting behavior of materials by using such machines [13]. However, using only an eccentric machine is of limited value because there are basic differences in the process of production on an eccentric and on a rotary tableting machine. Not all existing models are applicable to data from rotary machines. Pressure–time models have been mostly used to characterize compression processes on rotary machines because it is very difficult to measure punch travel on a rotary machine [9,10,14,15] and especially on high speed rotary machines. The three-dimensional modeling should be possible to apply to rotary machines when displacement measurement is easily available.

1.1.2. Rotary tableting machine simulation

The Presster (Fig. 2) [16,17], a single station rotary machine simulator, offers the possibility to measure time, force and displacement and to use only small amounts of material for formulation development. In the past, compaction simulators had been developed to mimic the processes happening on fast rotary machines, e.g. [18–22] and to test formulations with a small amount of material at high speed before running the actual tableting machine that usually consumes high amounts of material during testing. However, the use of these simulators has not always been satisfactory because it has been shown that it is not possible to mimic punch displacement travel and load profiles at the same time [17]. Nowadays, compaction simulators are mainly used for basic characterization of formulations and materials. They are now called ICRS (Integrated Compaction Research Systems). To mimic both displacement profiles and load profiles of a rotary machine, the Presster is a very useful equipment because it allows to mimic the compression process by mimicking the mechanics of a rotary machine; this means by using the same compression wheels used on rotary machines and the same geometries. The measurement of all three variables (time, force and displacement) enables the application of the new three-dimensional tableting technique.

1.2. Objective of the study

The aim of this study is therefore to apply this three-dimensional modeling technique to data gained by the rotary machine simulator and to offer a new possibility to improve tablet formulation development. The successful use of this model will not only help in basic material characterization, it will facilitate scale up during formulation and change of equipment during production.

2. Experimental part

2.1. Materials

The materials used were microcrystalline cellulose, MCC (Avicel® PH 101, Lot # 14204, FMC Corporation, Princeton, NJ), hydroxypropyl methylcellulose (HPMC 15.000, Metolose® 90 SH, Lot # 506825, Shin-Etsu, Tokyo, Japan), dicalcium phosphate dihydrate (Emcompress®, Lot # R 19 K, Mendell, Patterson, NY) and theophylline monohydrate (Lot # 4072.2, Roth GmbH, Karlsruhe, Germany).

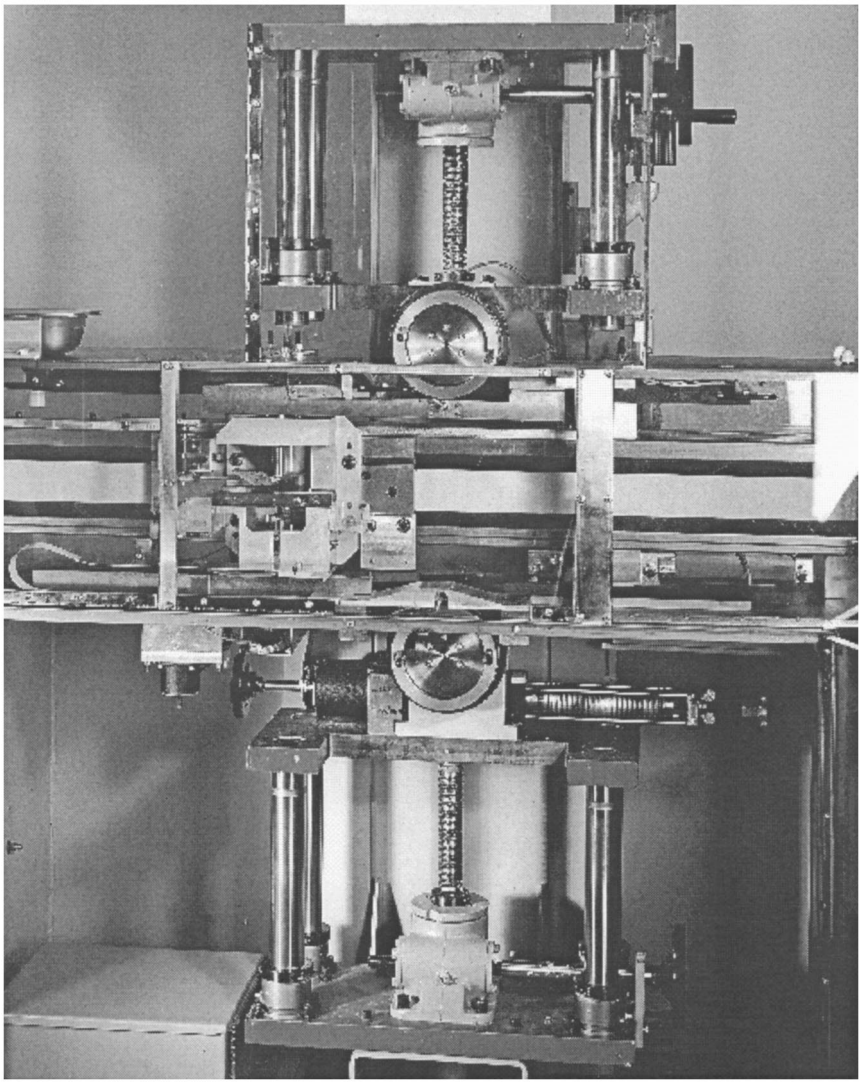

Fig. 2. The main compaction zone of the rotary tableting machine simulator, the Presster (© MCC Corporation, NJ).

Magnesium stearate (Lot # 93810410 Dr Caelo, Fröhlingsdorf, Germany) was used for internal lubrication.

2.2. Methods

2.2.1. Tableting

Tablets were produced on the Presster (Trademark of Metropolitan Computing Corporation, East Hanover, NJ), a single station rotary tableting machine simulator. The equipment is instrumented with inductive displacement transducers (Macro Sensors, Pennsauken, NJ) for the upper (Model: CD375-100) and the lower (Model: CD375-250) punch. The transducers were calibrated. Strain gages (N2A-06-T031P-350, Measurements Group Inc., Raleigh, NC) were applied at the upper compression roll pin. Measurement was temperature compensated. Calibration was performed up to 50 kN using a load cell (Model: 42/8378-01 s/n 331148 Sensotec, Columbus, OH). Compression rolls with the geometries of a Manesty Betapress were used for simulation. Dwell time was set to 10.2 ms referring to 100 rev./min of the original machine.

Standard PCT B tooling with 10 mm flat-faced punches was used throughout the study. Internal lubrication (0.5% magnesium stearate) was only used in case of dicalcium phosphate dihydrate. All other substances were tableted without lubrication to avoid its influence on material characteristics. Feeding of the die happened automatically using a feeding shoe with gravimetric force. The height of the tablets at the minimum distance between upper and lower punch was adjusted to 3 mm. The error for this determination was estimated to be 25 μm. The true densities of the substances were determined by gas pycnometry (Accupyc 1330, Micromeritrics, Norcross, GA) and are given in Table 1. Equal true volumes of the substances were tableted to the maximum relative densities ($\rho_{rel,\ max}$) 0.75, 0.80, 0.85, 0.90 and 0.95. The weight of the final tablets was recorded. The

Table 1
True densities of the materials[a]

Material	True density (g/cm^3)
Microcrystalline cellulose	1.580 (0.004)
Hydroxypropyl methylcellulose	1.331 (0.001)
Dicalcium phosphate dihydrate	2.331 (0.003)
Theophylline monohydrate	1.470 (0.002)

[a] Mean for $n = 3$. SD given in parentheses.

results are given in Tables 2–5. Before starting the study, the exact weight of the tablets was calculated from true density of the material, tablet height and the $\rho_{rel,\ max}$ to be tableted.

2.2.2. Data analysis

Force, time and displacement of the upper punch were recorded for each compaction cycle. Only data from tablets with the matching final weight and thickness during compression were used for further calculations. Data from five compaction cycles were used to calculate pressure and $\ln(1/1 - D_{rel})$ according to Heckel [1,2] with D_{rel} = relative density. The twisted plane with the equation given above was fitted to the calculated data.

Only the compression data above the 50% level of the maximum pressure were used for fitting. Since deformation of the particles mainly happens during the period of the compaction event it is regarded to be legitimate to use only this part of the data for comparison. The quality of the fits can be seen in Tables 2–5. A further loss of fitting quality using more data was not regarded as helpful. The parameters d, e and ω were used to describe and compare the tableting properties of the materials. The f was not interpreted because the influence of time and pressure cannot be differentiated.

3. Results and discussion

3.1. Fitting of the twisted plane

In Fig. 1 a three-dimensional plot of MCC is shown with displacement presented as $\ln(1/1 - D_{rel})$ according to Heckel, force presented as pressure and normalized time. This plot resulting from data obtained on the Presster by simulating a Manesty Betapress at 100 rev./min does no longer show the long dwell time characteristics typical for slow rotary machines [23]. This curve can be fitted with the twisted plane, which has been successfully used to characterize materials with an eccentric machine [13]. Fig. 3a–d show single fits performed as described in the experimental part for the different tableting substances MCC (Fig. 3a), HPMC (Fig. 3b), dicalcium phosphate dihydrate (Fig. 3c) and theophylline monohydrate (Fig. 3d). Fits from data tableted to the highest $\rho_{rel,\ max}$ of 0.95 are shown here to exhibit densification characteristics of the materials. The plots of MCC, HPMC and theophylline monohydrate show a positive angle of rotation, the plane has to be shifted upwards in the decompression part, while the plane fitted for dicalcium phosphate dihydrate is nearly flat. Thus, the twisting of the plane improves fitting by the rotation angle ω. Fig. 4 shows a typical example of a twisted plane with a negative angle of rotation. The decompression part is shifted downwards. Fig. 3a,c, MCC and dicalcium phosphate dihydrate, show a typical change during densification in one compaction cycle in the early stages of compaction. This is most obvious for dicalcium phosphate dihydrate. At lower densification, the particles mainly rearrange and fracture, while at higher densification they deform. Since only the data with pressures higher than 50% of the maximum pressure were used, the rearrangement of the particles is only of interest for the lower $\rho_{rel,\ max}$ where the quality of the fits is worse. Particle rearrangement, which happens in the early stages of compaction, is a more irregular process than deformation of a nearly completely formed tablet body.

3.2. Three-dimensional parameter plots

Fig. 5a,b and Tables 2–5 show the results of fitting for the different $\rho_{rel,\ max}$. Fig. 5 visualizes the change of the three-dimensional fitting at different $\rho_{rel,\ max}$. Usually, with increasing $\rho_{rel,\ max}$, the quality of the fits and the SD for the parameters is decreasing (Tables 2–5). The time dependent parameters d

Table 2
Tableting properties of microcrystalline cellulose[a]

Theoretical $\rho_{rel,\ max}$	0.75	0.80	0.85	0.90	0.95
Measured $\rho_{rel,\ max}$	0.747 (0.003)	0.801 (0.002)	0.850 (0.004)	0.899 (0.002)	0.950 (0.003)
Measured tablet height (mm)	3.004 (0.009)	3.006 (0.011)	3.002 (0.016)	2.996 (0.011)	3.004 (0.011)
Theoretical tablet weight (mg)	279.2	297.8	316.4	335.0	354.6
Measured tablet weight (mg)	278.4 (0.9)	298.8 (1.1)	316.8 (3.0)	334.4 (1.7)	354.0 (2.0)
Maximum pressure (MPa)	41.62 (3.03)	58.62 (2.54)	79.09 (1.13)	114.15 (2.10)	163.83 (1.54)
Quality of the fits (R^2)	0.00392 (0.00295)	0.00625 (0.00452)	0.00214 (0.00121)	0.00176 (0.00036)	0.00062 (0.00020)
Time plasticity (d)	0.6698 (0.1754)	0.6798 (0.531)	0.5768 (0.0624)	0.5769 (0.0409)	0.4885 (0.0118)
Pressure plasticity (e)	0.0103 (0.0024)	0.0078 (0.0010)	0.0050 (0.0006)	0.0034 (0.0003)	0.0020 (0.0001)
Intersection (f)	0.5340 (0.2143)	0.4868 (0.0886)	0.6016 (0.0860)	0.6138 (0.0376)	0.7372 (0.0226)
Angle of rotation (ω)	0.0112 (0.0034)	0.0085 (0.0040)	0.0090 (0.0008)	0.0049 (0.0018)	0.0036 (0.0006)

[a] Mean for $n = 5$. SD given in parentheses.

Table 3
Tableting properties of hydroxypropyl methylcellulose[a]

Theoretical $\rho_{rel,\ max}$	0.75	0.80	0.85	0.90	0.95
Measured $\rho_{rel,\ max}$	0.752 (0.003)	0.802 (0.001)	0.850 (0.003)	0.904 (0.004)	0.946 (0.003)
Measured tablet height (mm)	2.988 (0.023)	3.002 (0.008)	2.992 (0.019)	2.994 (0.011)	3.014 (0.009)
Theoretical tablet weight (mg)	235.2	250.9	266.5	282.2	297.9
Measured tablet weight (mg)	234.8 (1.0)	251.6 (0.9)	265.6 (1.7)	282.8 (2.3)	298.0 (1.4)
Maximum pressure (MPa)	18.93 (3.80)	27.15 (4.07)	38.02 (3.27)	68.35 (3.24)	95.09 (2.73)
Quality of the fits (R^2)	0.00331 (0.00353)	0.00413 (0.00395)	0.00174 (0.00125)	0.00077 (0.00030)	0.00017 (0.00014)
Time plasticity (d)	0.5807 (0.2625)	0.5950 (0.1170)	0.5631 (0.0462)	0.4209 (0.0213)	0.3665 (0.0028)
Pressure plasticity (e)	0.0147 (0.0050)	0.0135 (0.0034)	0.0083 (0.0024)	0.0054 (0.0003)	0.0034 (0.0004)
Intersection (f)	0.6073 (0.3530)	0.7286 (0.1385)	0.7416 (0.0647)	0.7693 (0.0243)	0.8331 (0.0095)
Angle of rotation (ω)	0.0210 (0.0249)	− 0.0041 (0.0060)	0.0027 (0.0036)	0.0086 (0.0011)	0.0072 (0.0018)

[a] Mean for $n = 5$. SD given in parentheses.

and ω show more error than e because at the tails of the force-time signal, the signal-to-noise ratio is smaller compared with the peak region of the curve. The target maximum tablet height and weight and thus the $\rho_{rel,\ max}$ were reached with acceptable error due to the mechanics of the Presster and some electrical noise. This shall be improved in further studies. The SD of force measurement is similar to eccentric tableting machines in comparison with the earlier study [13].

All materials show the highest values of e at the lowest $\rho_{rel,\ max}$ of 0.75. This means that with increasing $\rho_{rel,\ max}$ the plastic deformation due to pressure is decreasing. At lower $\rho_{rel,\ max}$, e is high as well when the particles rearrange and fracture as seen for dicalcium phosphate dihydrate (Fig. 5a). Up to a $\rho_{rel,\ max}$ of 0.85, e is decreasing. However, elastic decompression increases as seen by a decreasing ω – probably the total deformation remains similar. When this process has happened the newly formed particles, respectively, the tablet body deform plastically and this deformation takes time so that d is decreasing parallel to a slightly increasing e. This can be correlated to the strongly increasing maximum pressures at these $\rho_{rel,\ max}$.

The behavior of MCC is totally different (Fig. 5a). For MCC, parallel to a decreasing e d is decreasing. Further on, ω is decreasing. Thus, the percentage of plastic densification on the whole is decreasing. This material behaves more elastic depending on time and pressure. However, the maximum pressures at the different $\rho_{rel,\ max}$ are less increasing than for dicalcium phosphate dihydrate. MCC is known to show viscoelastic tableting behavior. The three-dimensional parameter plot visualizes this property. Compared with dicalcium phosphate dihydrate it is a much more plastically deforming material because d and e values are higher.

With increasing densification, HPMC (Fig. 5b) shows decreasing values of d and decreasing values of e. This behavior is similar to MCC, only compared with MCC, time plasticity is decreasing more and pressure plasticity less. The material needs more time and less pressure for densification than MCC at higher $\rho_{rel,\ max}$. ω behaves differently. At a $\rho_{rel,\ max}$ of 0.75 it is very low, the material shows a lot of fast elastic decompression. Then ω is e increasing up to the $\rho_{rel,\ max}$ of 0.90 and only at the highest $\rho_{rel,\ max}$ of 0.95 it is again low. This means that elastic decompression is decreasing and the decrease in plasticity (d and e) is balanced by an increase in ω. However, ω is in most cases lower than for MCC. At a $\rho_{rel,\ max}$ of 0.95 d, e and ω are decreasing. The materials show viscoleastic nature like MCC. Comparison of densification behavior at all $\rho_{rel,\ max}$ to MCC shows that the densification process is much less homogenous than that of MCC and to produce a tablet of good quality, high densification is necessary. This becomes also visible by higher SDs at the lower $\rho_{rel,\ max}$.

Theophylline monohydrate (Fig. 5b) shows a very irregu-

Table 4
Tableting properties of dicalcium phosphate dihydrate[a]

Theoretical $\rho_{rel,\ max}$	0.75	0.8	0.85	0.9	0.95
Measured $\rho_{rel,\ max}$	0.755 (0.003)	0.796 (0.002)	0.850 (0.001)	0.905 (0.002)	0.950 (0.003)
Measured tablet height (mm)	2.974 (0.005)	3.006 (0.005)	3.006 (0.017)	2.990 (0.014)	3.004 (0.005)
Theoretical tablet weight (mg)	411.9	439.3	466.8	494.3	521.7
Measured tablet weight (mg)	411.2 (1.8)	438.0 (0.0)	467.6 (3.0)	495.6 (3.6)	522.4 (0.9)
Maximum pressure (MPa)	47.75 (2.64)	72.14 (3.75)	138.56 (6.60)	255.86 (6.13)	414.98 (4.33)
Quality of the fits (R^2)	0.00138 (0.00061)	0.00067 (0.00055)	0.00083 (0.00046)	0.00023 (0.00011)	0.00051 (0.00014)
Time plasticity (d)	0.2513 (0.0597)	0.1882 (0.0536)	0.12415 (0.0196)	0.3115 (0.0231)	0.4567 (0.0195)
Pressure plasticity (e)	0.0073 (0.0012)	0.0040 (0.0008)	0.0023 (0.0015)	0.0007 (0.0001)	0.0005 (0.0000)
Intersection (f)	0.9301 (0.0796)	0.9808 (0.0619)	1.0564 (0.0463)	1.0116 (0.0108)	0.9018 (0.0141)
Angle of rotation (ω)	0.0131 (0.0027)	0.0097 (0.0016)	0.0064 (0.0030)	0.008 (0.0002)	− 0.0002 (0.0001)

[a] Mean for $n = 5$. SD given in parentheses.

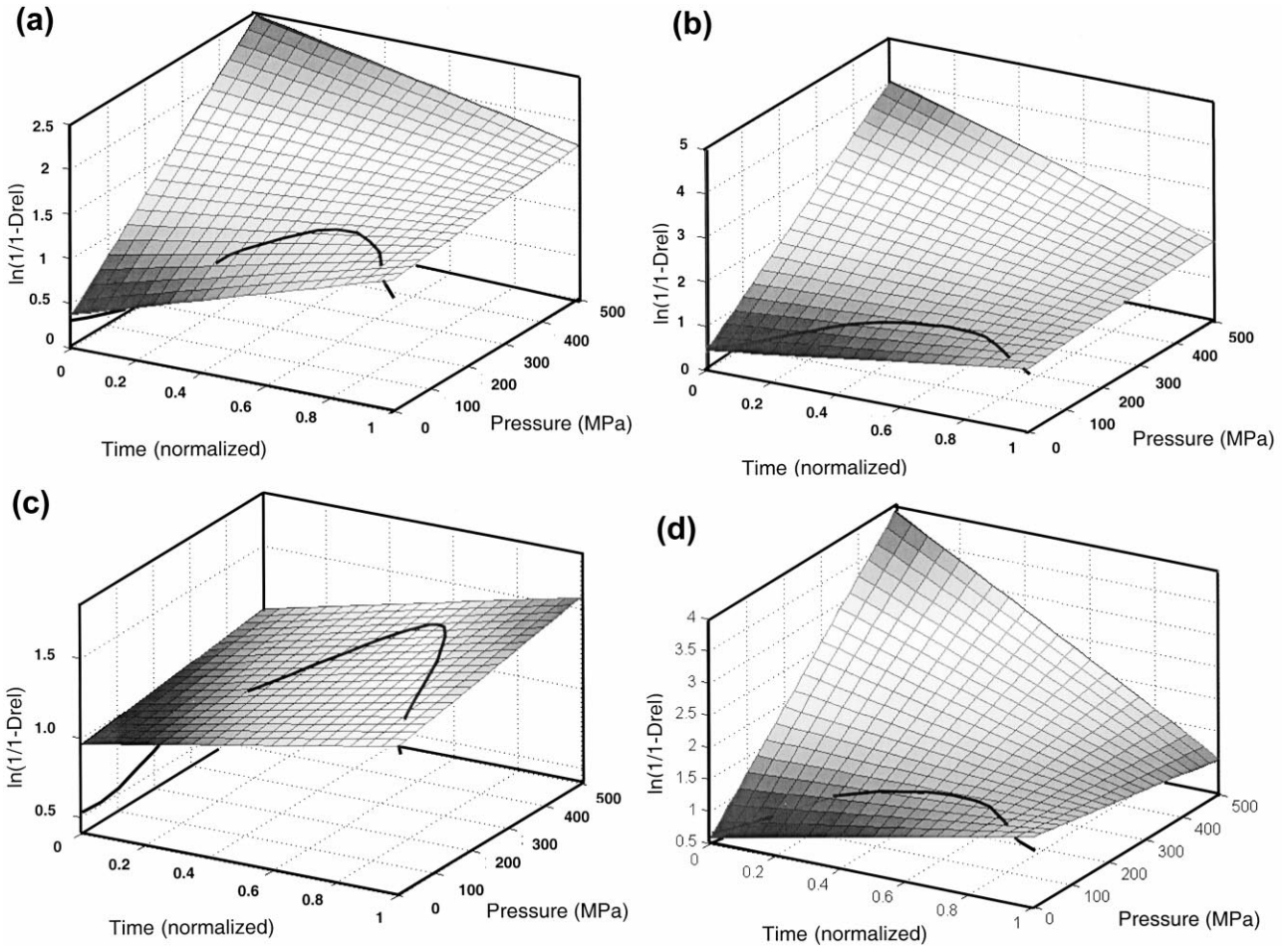

Fig. 3. Three-dimensional data-plot for one compaction cycle of (a) microcrystalline cellulose, (b) hydroxypropyl methylcellulose, (c) dicalcium phosphate dihydrate and (d) theophylline monohydrate at a $\rho_{rel,\ max}$ of 0.95 with a fitted plane according to the three-dimensional model (Eq. (1)).

lar shape of the three-dimensional parameter plot. The error of the fits and the SDs are quite high. This is partially due to the low pressures which this material needs for densification. It shows a continuous decrease of d with increasing $\rho_{rel,\ max}$ – much more than for MCC and HPMC. Simultaneously, a strong increase in ω up to a $\rho_{rel,\ max}$ of 0.85 can be seen. As for HPMC, elastic decompression is decreasing. Then, when the tablet is formed, and the whole tablet body reacts as a body, e is strongly decreasing, ω is decreasing and d is decreasing. The formed body resists densification and more time and pressure is needed for densification – it is less plastic. However, this material is more plastic than MCC and HPMC because the ω values are a lot higher.

3.3. Comparison with application from an eccentric tableting machine

The parameter values for the fits with the compaction cycles of the Presster are different compared with those of an eccentric machine because the time for the compaction event and the performance of the tableting process are different. This is mainly due to the mechanics, which are different between eccentric and rotary tableting machines. Especially the parameter d is affected because the tableting event takes on rotary machines the same time for all the

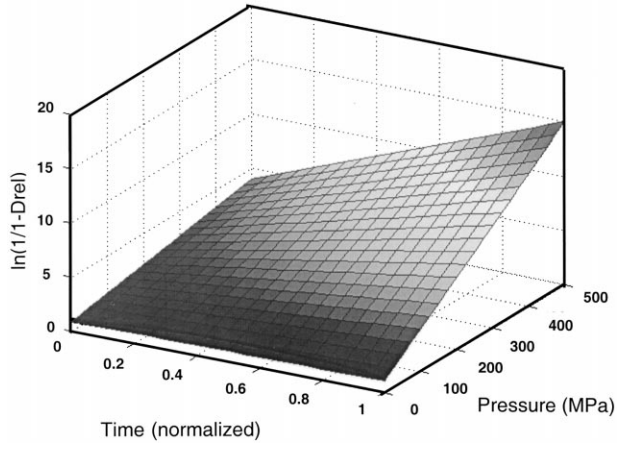

Fig. 4. Three-dimensional data-plot for one compaction cycle of hydroxypropyl methylcellulose at a $\rho_{rel,\ max}$ of 0.75 with a fitted plane according to the three-dimensional model (Eq. (1)).

Table 5
Tableting properties of theophylline monohydrate[a]

Theoretical $\rho_{rel,\ max}$	0.75	0.80	0.85	0.90	0.95
Measured $\rho_{rel,\ max}$	0.753 (0.004)	0.794 (0.004)	0.847 (0.004)	0.901 (0.004)	0.954 (0.002)
Measured tablet height (mm)	3.002 (0.016)	3.004 (0.011)	3.016 (0.011)	3.008 (0.023)	2.986 (0.045)
Theoretical tablet weight (mg)	259.7	277.1	294.4	311.6	329.0
Measured tablet weight (mg)	260.8 (1.8)	275.2 (1.1)	295.0 (2.3)	312.8 (1.8)	328.8 (4.8)
Maximum pressure (MPa)	10.44 (6.03)	21.87 (7.31)	38.92 (7.60)	67.33 (8.36)	113.09 (8.29)
Quality of the fits R^2	0.00099 (0.00067)	0.00530 (0.00797)	0.00462 (0.00131)	0.00149 (0.00073	0.00247 (0.00097)
Time plasticity (d)	0.5666 (0.1414)	0.4550 (0.1788)	0.3773 (0.1378)	0.2518 (0.0688)	0.1637 (0.0664)
Pressure plasticity (e)	0.0156 (0.0039)	0.0088 (0.0048)	0.0109 (0.0032)	0.0049 (0.0009)	0.0024 (0.0009)
Intersection (f)	0.8719 (0.4540)	0.9865 (0.2753)	0.7406(0.0740)	0.9065 (0.0552)	1.0453 (0.1249)
Angle of rotation (ω)	− 0.0213 (0.0205)	− 0.0022 (0.0105)	0.0177 (0.098)	0.0117 (0.0020)	0.0066 (0.0003)

[a] Mean for $n = 3$. SD given in parentheses.

materials, contrary to the compaction event happening in eccentric tableting machines. The parameters e and ω are affected by the shape of the curves. Thus, the three-dimensional parameter plots look different. However, the results show that an evaluation of the tableting process with the three-dimensional model is very useful for rotary machines as well.

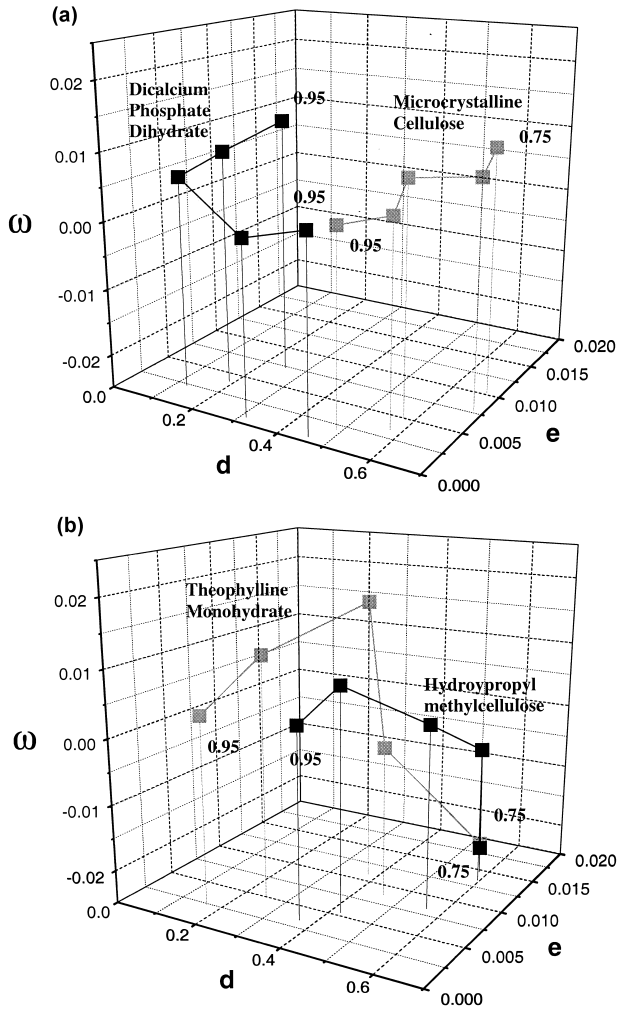

Fig. 5. Parameter plot for different tableting materials at different graded $\rho_{rel,\ max}$ 0.75, 0.80, 0.85, 0.90 and 0.95 (a) microcrystalline cellulose and dicalcium phosphate dihydrate and (b) theophylline monohydrate and hydroxypropyl methylcellulose.

4. Conclusions

With the use of the rotary tableting machine simulator Presster, it is possible to apply the new three-dimensional modeling technique to compaction data similar to those of rotary machines. The results of three-dimensional modeling show that the technique can be used on very different types of equipment, which is necessary in scale-up and production of tablets. Thus, three-dimensional modeling of tableting data is a valuable tool not only for basic material characterization on eccentric tableting machines but on rotary tableting machines as well.

Acknowledgements

Thanks a lot to MCC Corporation, East Hanover, NJ, for the practical performance of the studies with the Presster and valuable discussions, especially to Lev Tsygan for tableting and to Michael Levin for reading the manuscript.

References

[1] R.W. Heckel, An analysis of powder compaction phenomena, Trans. Metall. Soc. AIME 221 (1961) 1001–1008.
[2] R.W. Heckel, Density-pressure relationships in powder compaction, Trans. Metall. Soc. AIME 221 (1961) 671–675.
[3] C. Fuehrer, Über den Druckverlauf bei der Tablettierung in Exzenterpressen, Dtsch. Apoth. Ztg. 102 (1962) 827–832.
[4] M. Dürr, D. Hanssen, H. Harwalik, Kennzahlen zur Beurteilung der Verpreßbarkeit von Pulvern und Granulaten, Pharm. Ind. 34 (1972) 905–911.
[5] H. Moldenhauer, H. Kala, G. Zessin, M. Dittgen, Zur pharmazeutischen Technologie der Tablettierung, Pharmazie 35 (1980) 714–726.
[6] G. Ragnarsson, J. Sjogren, Force displacement measurements in tableting, J. Pharm. Pharmacol. 37 (1985) 145–150.
[7] R. Dietrich, J.B. Mielck, Parametrisierung des zeitlichen Verlaufs der

Verdichtung bei der Tablettierung mit Hilfe der modifizierten Weibull-Funktion, Pharm. Ind. 47 (1985) 216–220.

[8] J.B. Mielck, G. Stark, Tableting of powder mixtures: Parameters of evolved pressure–time profiles indicate percolation thresholds during tableting, Eur. J. Pharm. Biopharm. 41 (1995) 206–214.

[9] P.C. Schmidt, U. Tenter, Force and displacement characteristics of rotary tableting machines, Pharm. Ind. 49 (1987) 637–642.

[10] P.C. Schmidt, U. Tenter, Presskraft- und Weg-Zeit-Charakteristik von Rundlauftablettenpressen, 3.Mitt.: Vergleich verschiedener Pressmaterialien, Pharm. Ind. 50 (1988) 376–381.

[11] E.G. Rippie, D.W. Danielsson, Viscoelastic stress/strain behaviour of pharmaceutical tablets: analysis during unloading and postcompression periods, J. Pharm. Sci. 70 (1981) 476–482.

[12] F. Müller, Viscoelastic models, in: G. Alderborn, C. Nyström (Eds.), Pharmaceutical Powder Compaction Technology, Marcel Dekker Inc, New York, 1995, pp. 99–132.

[13] K.M. Picker, A new theoretical model to characterize the densification behavior of tableting materials, Eur. J. Pharm. Biopharm. 49 (2000) 267–273.

[14] D.W. Danielson, W.T. Morehead, E.G. Rippie, Unloading and postcompression viscoeleastic stress versus strain behavior of pharmaceutical solids, J. Pharm. Sci. 72 (1983) 342–345.

[15] C. Matz, A. Bauer-Brandl, T. Rigassi, R. Schubert, D. Becker, On the accuracy of a new displacement instrumentation for rotary tablet presses, Drug Dev. Ind. Pharm. 25 (1999) 117–130.

[16] M. Levin, L. Tsygan, S. Dukler, Press simulation apparatus and methods, US Patent application No. 08/998,536 International Patent application No. PCT/US98/27421, filed December 23, 1998.

[17] M. Levin, Theory and practice of tablet press simulation for process scale-up, Arden House Conference, January, 1999.

[18] M. Celik, K. Marshall, Use of a compaction simulator system in tableting research, Drug Dev. Ind. Pharm. 15 (1989) 759–800.

[19] S.D. Bateman, M.H. Rubinstein, R.C. Rowe, R.J. Roberts, P. Drew, A.Y.K. Ho, A comparative investigation on compression simulators, Int. J. Pharm. 49 (1989) 209–212.

[20] S.D. Bateman, High speed compaction simulators in tabletting research, Pharm. J. 240 (1988) 632–633.

[21] L.E. Holman, K. Marshall, Calibration of compaction simulator for the calibration of tablet thickness during compression, Pharm. Res. 10 (1993) 816–822.

[22] C.D. Ruegger, An investigation of the effect of compaction profiles on the tableting properties of pharmaceutical substances, PhD Thesis, Rutgers University, 1996.

[23] P. Konkel, J.B. Mielck, Associations of parameters characterizing the time course of the tableting process on a reciprocating and on rotary tableting machine for high-speed production, Eur. J. Pharm. Biopharm. 45 (1998) 137–148.